# Use of the cantilever beam vibration method for determining the elastic properties of maritime pine cross-laminated panels

Gian Felice Giaccu[a,*], Daniel Meloni[b], Giovanna Concu[b], Monica Valdes[b],

Massimo Fragiacomo[c]


[a]*Department of Architecture, Design and Urban Planning, University of Sassari,*

*Alghero, Italy.*

[b]*Department of Civil and Environmental Engineering and Architecture, University of Cagliari,*

*Cagliari, Italy.*

[c]*Department of Civil, Construction-Architectural &Environmental Engineering, University of*

*L'Aquila, L'Aquila, Italy.*

**Abstract**

This paper presents a study aimed to assess the modulus of elasticity $E_0$ and the rolling shear modulus $G_{90}$ of three-layer Maritime Pine Cross Laminated Timber (CLT) panels. The proposed methodology is based on a vibration test carried out on panels in cantilever configuration and on the results of a sensitivity study conducted via FE model analyses, which highlights a straightforward relationship between the first two vertical natural frequencies and the aforementioned elastic properties of the panels. The procedure has been developed and applied to a specific configuration of CLT panels made of Sardinian Maritime Pine (Pinus Pinaster). Nevertheless, the same approach could be easily extended to any cantilever three layers CLT panel with different dimensions, providing a new sensitivity study is carried out. The results suggest that the proposed methodology can be effectively used as a dynamic identification process for quality control in industrial production chains, where the role of non-destructive controls is becoming increasingly important.

**1. Introduction**

Cross Laminated Timber (CLT) is a promising and relatively new wood-based structural product which is increasingly used on the building market for the several advantages it can offer [1]. CLT panels are wooden structural products consisting of laminations of finger-jointed boards, arranged crosswise and glued together according to different lay-ups. This cross-lamination process brings several structural advantages including: stability of long panels with respect to swelling and shrinkage, reduced scatter of original lumber properties, reduced influence of anatomic defects, two-way behavior in slabs, and relatively high transverse and in-plane stiffness [2].

CLT technology is particularly suitable for modular buildings, since it can be employed in horizontal elements (floors and roofs) and vertical load-bearing systems (wall panels),according to different structural and finishing quality design [3]. CLT panels allow for large spans and good behavior with respect to fire [4] and earthquake resistance [5,6]; moreover, the ease of installation of modular systems ensures the effectiveness of the construction process [7].

On the other hand, the use of CLT technology requires careful consideration of serviceability design, including deflection control [8] due to low bending stiffness, high creep and shrinkage deformations [9-11]. Furthermore, vibration control may be an issue, as well as possible low acoustic insulation properties [12] due to low mass of wood. Therefore, additional timber layers have sometimes to be used to increase stiffness and acoustic separation [13-15]. The assessment of the elastic mechanical properties of CLT panels thus represents a crucial issue for a proper design of CLT buildings.

The linear model [16] is generally used in CLT design as the plasticization of timber in compression is usually negligible. However, in the case of reinforced elements more complex non-

1 linear three-dimensional models can be used [17]. Furthermore, new studies have focused on

2 modeling the flexural behavior of hybrid timber-steel and timber-concrete beams through

3 sophisticated non-linear models [18,19]. Since the goal of this paper is the evaluation of global

4 elastic properties of CLT panels, a linear constitutive model has been considered throughout the

5 numerical investigation.

6 The mechanical behavior of CLT is rather complex due to the intrinsic anisotropy of timber,

7 its anatomic defects and the cross-wise arrangement of panel layers. Significant variations in

8 mechanical properties can be noticed in CLT depending on the layers orientation [20,21]. This fact

9 can be ascribed to the dramatic difference between the Young's modulus of the boards parallel

10 ($E_0$) and perpendicular ($E_{90}$) to the grain direction, and the shear moduli of the boards in the parallel

11 (longitudinal shear modulus $G_0$) and orthogonal planes (rolling shear modulus $G_{90}$), the latter being

12 usually very small. This issues can cause a mechanical complexity in CLT panels which may be

13 not effectively tackled by using the standard beam theory [16,22].

14 In this respect, several analytical approaches have been presented in literature for the

15 evaluation of an effective or equivalent bending stiffness depending on timber layers elastic

16 properties, thickness and grain orientation [16,23,24]. The most referenced ones are: the

17 "Mechanically jointed Beams Theory", or γ-method (GM), proposed in the Annex B of Eurocode

18 5 [24], the "Composite Theory", or k-method (KM) [25] and the "Shear Analogy Method"(SAM)

19 [26]. Recently, Thiel et al. proposed a Timoshenko beam approaches a simplified alternative

20 [2,23].

21 Several authors proposed innovative approaches in order to take the influence of shear into

22 account for composite elements. As an example, Kaci et al. [27] developed an exact analytical

23 solution for the analysis of the post-buckling non-linear response of simply supported deformable

1 symmetric composite beams. Kada et al. presented in [28] the results of a static flexure analysis of

2 laminated composite plates by utilizing a higher order shear deformation theory in which the

3 stretching effect is incorporated. Moreover, the vibrations and bending responses of carbon

4 nanotube-reinforced composite plates resting on the Pasternak elastic foundation are analyzed in

5 [29]. Belabed et al. [30] and Zidi et al. [31] discussed new hyperbolic plate theory for the free

6 vibration analysis of functionally graded material (FGM) sandwich plates. Zine et al. [32] and

7 Chikh [33] performed the bending and free vibration analysis of multilayered plates and shells,

8 and a thermal buckling analysis of cross-ply laminated composite plates, respectively, by utilizing

9 a new higher order shear deformation theory (HSDT). They also compared the results of their

10 approach against existing theories for investigating the static and dynamic response of isotropic

11 and multilayered composite shell and plate structures and the thermal buckling behavior of

12 laminated composite plates. Moreover advanced theories which take into account of the shear

13 deformation effects on beams and plates are discussed in the recent works [34-36].

14 The experimental determination of wood products elastic properties can be performed using

15 different methodologies. Either destructive or non-destructive techniques can be used for the

16 determination of elastic properties of CLT panels [37]. However, some of these properties, like the

17 aforementioned rolling shear modulus $G_{90}$, are currently determined via empirical correlations

18 with other properties such as the longitudinal elastic modulus $E_0$, since their direct evaluation

19 requires special tests and measurement equipment [37]. The indirect evaluation of elastic

20 properties of CLT elements is therefore important and represents one of the goals of this paper.

21 In recent years researchers have focused the attention on non-destructive techniques [38-40]

22 and several dynamic testing methods have been proposed for the determination of both elastic and

23 shear moduli of wood composite panels. Dynamic testing has been proved to be an effective

1 procedure for performing elastic identification of CLT panels [41-43] and cantilever beam

2 vibration methods have been listed as reliable approaches in [42,43]. Nevertheless, these

3 approaches are usually based on a Euler-Bernoulli beam analysis [41], which can lead, as

4 illustrated in [41,44], to systematic errors in evaluating the CLT panel elastic modulus $E_0$, and to

5 disregard the role of shear deformations. In this respect, the determination of the rolling shear

6 modulus is commonly based on static tests, in accordance with EN 408 [45]. However, as

7 previously mentioned, a rather complex experimental set-up is required to carry out the tests.

8 Furthermore, when applied to CLT panels, these approaches may lead to localized measurements

9 usually not representative of the global elastic behavior of the specimens due to the intrinsic

10 heterogeneity of the CLT panels [20].

11 This paper illustrates an innovative dynamic identification procedure, developed for three-

12 layer CLT panels, and based on the results of sensitivity analyses performed by means of a 3D

13 solid Finite Element (FE) model. The proposed procedure enables the determination of the main

14 elastic properties of laminations forming the CLT specimen, including the dynamic modulus of

15 elasticity ($E_0$) and the dynamic rolling shear modulus ($G_{90}$).

16 The paper is organized as follows: Section 2 illustrates the theoretical background regarding

17 the beam theory and the FE model approach; Section 3 describes the tested specimens, the related

18 sensitivity analyses and the dynamic identification procedure; numerical results are discussed in

19 Section 4;conclusions are summarized in Section 5.


20 **2. Theoretical background**

21 The proposed methodology is based on a set of sensitivity analyses, performed using the FE

22 model illustrated in Section 2.2, aimed at the indirect determination of the elastic properties.

23 Nevertheless, as a comparison tool, a free vibration approach based on Euler-Bernoulli beam

1  theory is discussed in Section 2.1. The comparison between classic beam theories and FE models

2  can be a useful mean for understanding the limits of the Euler-Bernoulli beam approach [16] often

3  employed in dynamic identification techniques [41,43] and in structural design of timber

4  construction.

5  2.1 *Free vibration Euler Bernoulli beam theory*

6  The theoretical relationship between the dynamic modulus of elasticity (MOE) parallel to the

7  grain orientation of face boards and the first natural vibration frequency *f* of the panel can be

8  assessed using the cantilever beam free vibration theory, provided a proper transformed moment

9  of inertia is employed; for this configuration the dynamic MOE can be calculated through the

10  following formula [46]:

11  $$E_0 = (2\pi f)^2 \frac{M}{LI} \left(\frac{l}{1.875}\right)^4 \tag{1}$$

12  where $E_0$ (Pa) is the dynamic MOE of the panel parallel to the grain orientation of face boards, *f*

13  (Hz)is the panel first natural vibration frequency, *M* (kgf) is the weight of the specimen, *L* (m) is

14  the length of the panel, $I$ (m$^4$)is the cross-section effective moment of inertia with respect to the

15  centroid, while *l* (m) denotes the effective span of the cantilever [16,43]. The panel MOE can

16  therefore be easily evaluated through an experimental determination of the first natural frequency.

17  Regarding the evaluation of the effective bending stiffness, since the CLT panel cross-section

18  consists of differently (usually 0°/90°) oriented and mutually glued layers, the following issues

19  need to be considered. Firstly, the 90° oriented layers offer a minimum contribution to the panel

20  longitudinal bending stiffness due to the low value of $E_{90}$ compared to $E_0$ (usually a ratio $E_{90}/E_0 =$

21  1/30 [24] is assumed for softwood). Secondly, for low slenderness elements, bending deformations

22  are considerably affected by the shear stiffness and in particular, by the rolling shear modulus of

7

1  inner 90° oriented layers, which is conventionally assumed as 1/10 of the longitudinal shear

2  modulus $G_0$ [24]. Analytical models for the evaluation of an actual or equivalent bending stiffness

3  depending on layers elastic properties, thickness and grain orientation have already been

4  mentioned in Section 1. Among them, only GM and SAM can handle shear deformations, while

5  *KM* only accounts for bending stiffness and thus, it should be used only for high span-to-depth

6  (*L/H)* panel ratios. In the following, Eq. (1) is employed with an effective moment of inertia

7  evaluated using the transformed section method, assuming $E_{90}/E_0$=1/30, and neglecting the

8  influence of the shear deformation.


9  2.2  *Finite Element model*

10  This section describes the adopted FE model, which represents an improved tool for an accurate

11  dynamic modeling of the CLT panels, directly depending on the elastic properties of the boards

12  forming the panel layers. For this purpose, a 3D model has been implemented in Abaqus 2017

13  software package and a numerical investigation has been carried out. The model is characterized

14  by a structured mesh of 80640 isoparametric brick elements (7,5x5x5 mm), selected after a

15  convergence test with subsequent mesh refining, until a variation threshold of the higher frequency

16  smaller than 1% was achieved. Despite the small grooves in each lamination boards and the vertical

17  gaps in the inner layer introduced during production to prevent excessive cupping and cracking,

18  full continuity between the layers has been assumed in the FE mesh. As shown in a previous work

19  [2], such grooves and gaps do not considerably affect the overall panel behavior. Similarly, the

20  presence of the glue film among timber layers has been neglected, since it does not affect the panel
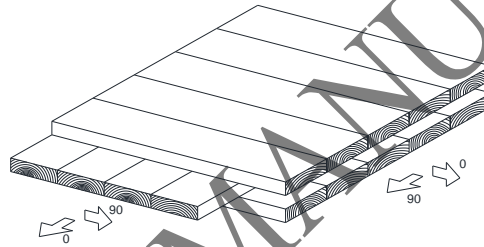
21  deformations.

22  As a result of its anatomy, timber shows an anisotropic constitutive behavior, usually regarded

23  as orthotropic, which is based on a grain-oriented orthogonal system for each timber layer, as if

8

1 growth rings were flattened. This assumption introduces a certain conventionality in the modeling.

2 Therefore, only the following five elastic parameters have been accounted for in the constitutive
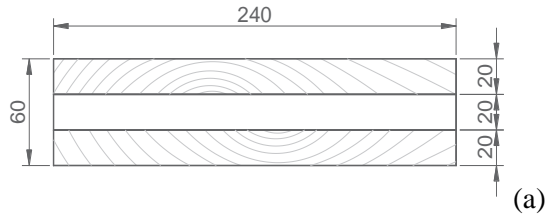
3 model:

4
$$E_l = E_0, \; E_t = E_r = E_{90}, \; G_{lr} = G_{lt} = G_0, \; G_{rt} = G_{90}, \; \nu_{lr} = \nu_{lt} = \nu_{rt} = \nu \tag{2}$$
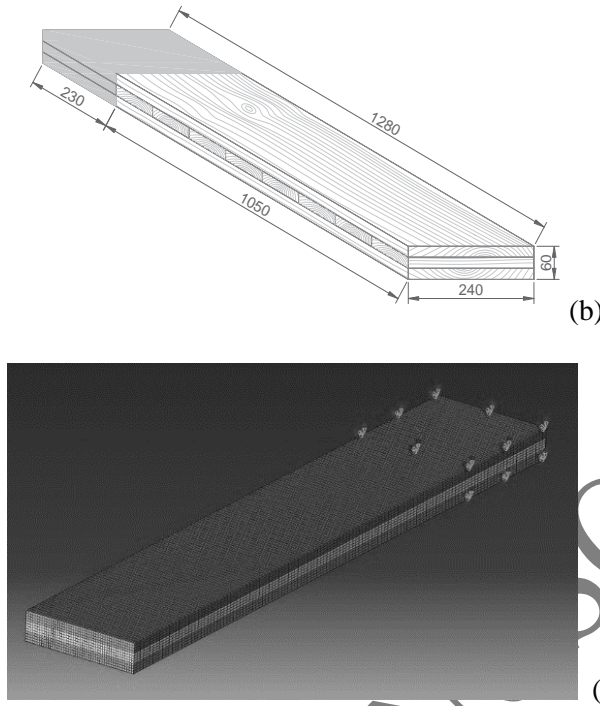
5 where the subscripts *l, t* and *r* signify the longitudinal, the tangential and the radial directions

6 respectively. Given the above assumptions, the layer orientations in the panel layup have been

7 modeled by rotating the lamination local material orientations according to the 0°/90° panel

8 directions as shown in Fig. 1.

9



10 **Fig. 1.** Schematic of the three layers CLT panel.

11 The cantilever configuration has then been modeled by imposing zero displacement boundary

12 conditions at the fixed edge of the specimen, as shown in Fig. 2b, in accordance with the

13 experimental set-up.

14



(a)

1



2

3　**Fig. 2.**(a) Cross section of 60PF specimens (60×240×1280 mm),(b) schematic of the experimental set-up,
4　(c) FEM model of three layers cantilever CLT specimen.

## 3. Material and methods

6　3.1 *Specimens and testing program*

7　The investigated CLT panels are composed by three layers of solid timber finger-jointed

8　boards, previously graded, crosswise packed (0°-90°-0°) and glued together. For this study, a total

9　number of 14 panels 240 mm wide, 60 mm thick and 1280 mm long, made of Sardinian Maritime

10　Pine (Pinus Pinaster) has been used. The panels (60-PF series) are made of 20 mm thick boards,

11　with a global panel thickness of 60 mm. The cross-section geometry of the 60PF series panels is

12　shown in Fig.2a. Maritime Pine boards have been previous classified, according to EN 338 [47]

13　strength classes, as C16 and C14 for the outer and the inner layers respectively. Classification is

14　based on the visual grading rule recently developed by the Department of Civil, Environmental

15　Engineering and Architecture (DICAAR) of the University of Cagliari [48,49], in cooperation with

1   the CNR-IVALSA of Florence. Table1 lists the main properties of the tested panels. The specimen

2   has been rigidly clamped for a length of 230 mm in cantilever position with a free span of 1050

3   mm as illustrated in Fig.2.

4   **Table 1**
5   Specimen dimensions, weight and density.

| Specimen code | $B$ (Breadth) [mm] | $H$ (Depth) [mm] | $L$ (Length) [mm] | Weight [g] | Mean Density [kg/m$^3$] |
|---|---|---|---|---|---|
| 60PF 8 | 2460.50 | 62.09 | 1280.00 | 8759.50 | 4480.12 |
| 60PF 9 | 2427.00 | 61.87 | 1279.00 | 9048.00 | 4711.85 |
| 60PF 10 | 2430.00 | 61.80 | 1280.00 | 9131.50 | 4750.48 |
| 60PF 11 | 2437.00 | 62.44 | 1280.00 | 9503.50 | 4880.20 |
| 60PF 12 | 2435.50 | 61.88 | 1279.00 | 9634.00 | 4999.31 |
| 60PF 13 | 2450.00 | 61.76 | 1280.00 | 9018.00 | 4656.15 |
| 60PF 14 | 2467.00 | 61.83 | 1280.00 | 8997.00 | 4608.94 |
| 60PF 15 | 2420.50 | 61.85 | 1279.00 | 9592.50 | 5010.79 |
| 60PF 16 | 2457.50 | 61.54 | 1280.00 | 8812.00 | 4553.91 |
| 60PF 17 | 2460.00 | 61.59 | 1280.00 | 9736.50 | 5020.24 |
| 60PF 18 | 2430.00 | 61.77 | 1280.00 | 8645.00 | 4499.33 |
| 60PF 19 | 2430.00 | 61.96 | 1280.00 | 9323.00 | 4837.58 |
| 60PF 20 | 2430.50 | 62.01 | 1280.00 | 9504.50 | 4927.78 |
| 60PF 21 | 2417.50 | 62.29 | 1280.00 | 9188.00 | 4768.18 |

6

7   3.2  *Sensitivity analysis (numerical modeling)*

8       A comprehensive set of sensitivity analyses aimed to assess the global dynamic behavior of the

9   panels depending upon the material elastic properties has been carried out.

10      The dimensions of the 60-PF specimens have been chosen according to the commercial

11  thickness of the boards forming the panel (20mm), with a Length-to-Depth ratio (*L/H*) high enough

12  to ensure that the shear deformation can be regarded as negligible in cantilever configuration.

13      The analyses have been specifically conducted for the 60-PF specimen type illustrated in Fig.2

14  and are therefore fully reliable only for that configuration; nevertheless the same approach could

15  be easily extended to any cantilever three-layer CLT specimen with different dimensions, by

16  means new sensitivity studies. Similar trends of sensitivity analyses are expected for this case.

11

The proposed methodology has been applied to a benchmark model having the initial elastic properties shown in Table 2 and evaluated as function of $E_0$, according to EN384 [50] ($E_{90}= E_0/30$, $G_0= E_0/16$, $G_{90}= G_0/10$ and $v= 0.40$).

**Table 2**
Values of initial elastic properties of the benchmark model.

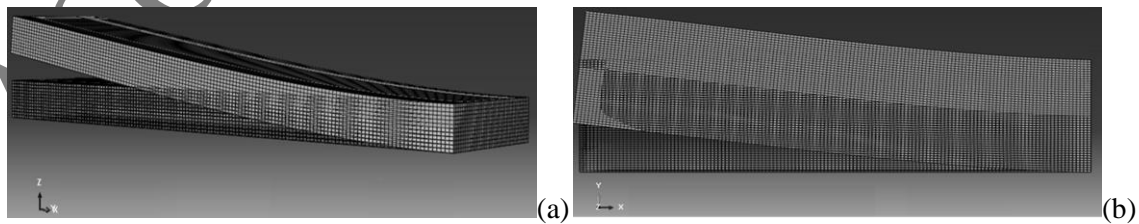| $E_0$ [MPa] | $E_{90}$ [MPa] | $G_0$ [MPa] | $G_{90}$ [MPa] | $v$ [-] |
|---|---|---|---|---|
| 7500.00 | 250.00 | 468.75 | 46.88 | 0.40 |

The analyses have been conducted for the first four natural frequencies by varying the elastic properties in a suitable range, displayed in Table 3; the natural frequencies have been assessed as function of each considered property, by varying the elastic properties once at a time while keeping the other elastic properties constant to the initial values displayed in Table 2.
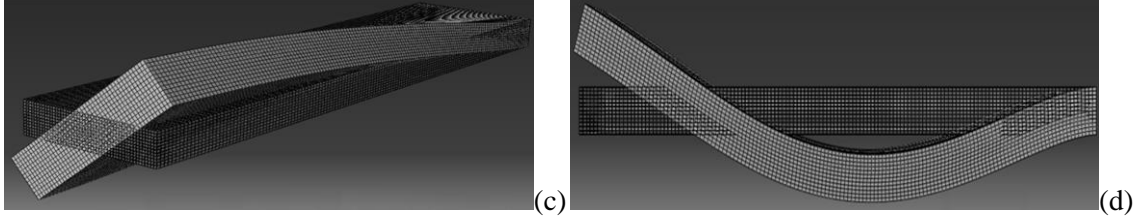
**Table 3**
Values of elastic properties range accounted for the sensitive analyses.

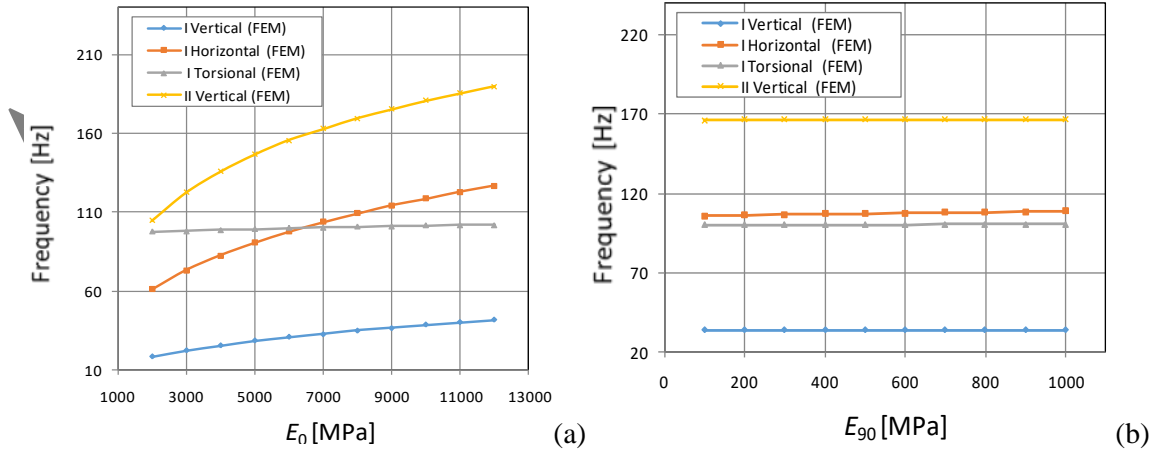| $E_0$ [MPa] | $E_{90}$ [MPa] | $G_0$ [MPa] | $G_{90}$ [MPa] | $v$ [-] |
|---|---|---|---|---|
| 2000-12000 | 100-1000 | 200-1000 | 20-150 | 0.40 |

Figure 3 shows the first four mode shapes obtained by the FE model of the specimens in cantilever configuration.
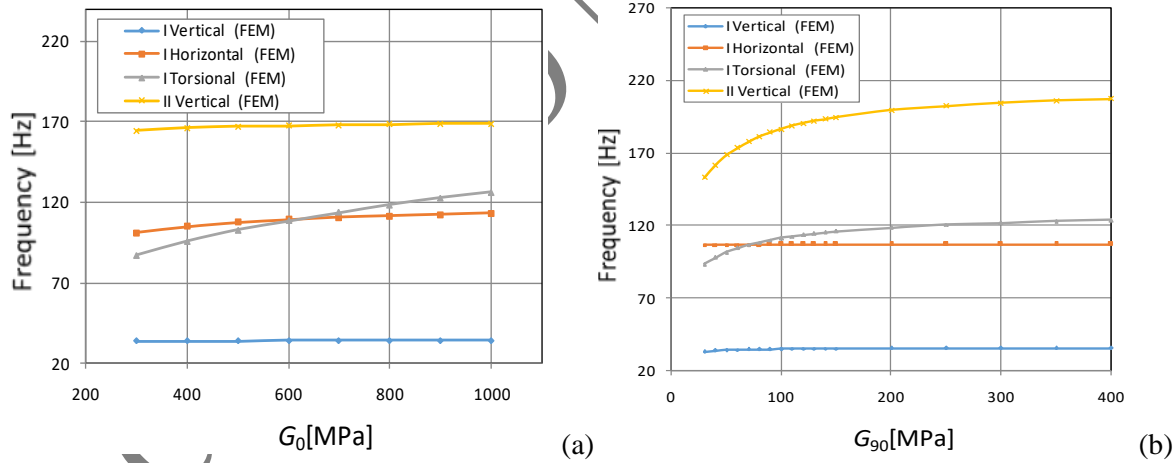


(a)　　　　　　　　　　　　　　　(b)

(c)   (d)

**Fig. 3.** Mode shapes of the specimens in cantilever configuration (FE): (a) first vertical mode, (b) first horizontal mode, (c) first torsional mode, (d) second vertical mode.

The results of the sensitivity analyses are displayed in Figs.4-5. Figure 4 shows the natural frequencies of the specimens as a function of $E_0$ (Fig. 4a) and $E_{90}$ (Fig. 4b). The elastic properties affect the global dynamic behavior differently with respect to the different vibration modes. Fig.4a reveals that $E_0$ affects the vertical and horizontal modes but not the torsional one; on the other hand, it is noteworthy that $E_{90}$ does not have any influence in the four examined modes (Fig.4b), by varying the parameters in the whole examined range. This result can be justified by observing that $E_{90}$ is not exploited in any of the considered modes, with exception of the central layer which, on the other hand, provides a minor contribution to the overall panel stiffness due to its proximity to the neutral axis. Moreover, $E_{90}$ values are much lower with respect to $E_0$. This result confirms the possibility to simply neglect the central layer in the evaluation of the effective bending stiffness as commonly done in current design procedures.



(a)   (b)

13

**Fig. 4.** Natural frequencies of the specimens as function of elastic properties (FEM) of the benchmark model:(a) $E_0$ and (b) $E_{90}$.

Figure 5 displays the natural frequencies of the specimens depending upon $G_0$ (Fig. 5a) and $G_{90}$ (Fig. 5b) variations; $G_0$ directly affects horizontal and torsional modes, hardly influences the second vertical mode and does not affect the first vertical mode at all. Conversely, the second vertical mode, which is almost independent of $G_0$, is markedly influenced by $G_{90}$ (Fig. 5b). This occurrence can be explained by the high slenderness of the panels (Length-to-Depth ratio $L/H=$ 17.5), which makes shear deformations negligible for the first vertical mode; on the other hand, for a lower Length-to-Breadth ratio ($L/B=$ 4.4), the first horizontal mode shows a clear dependency by on $G_0$. Conversely, shear clearly affects the second vertical mode (bending mode), but due to the low $G_{90}/G_0$ ratio, in this case deformations are mostly governed by rolling shear deformations in the central layer rather than longitudinal shear deformations in the outer layers.



(a)

(b)

**Fig. 5.** Natural frequencies of the specimens as function of elastic properties (FEM) of the benchmark model: (a) $G_0$ and (b) $G_{90}$.
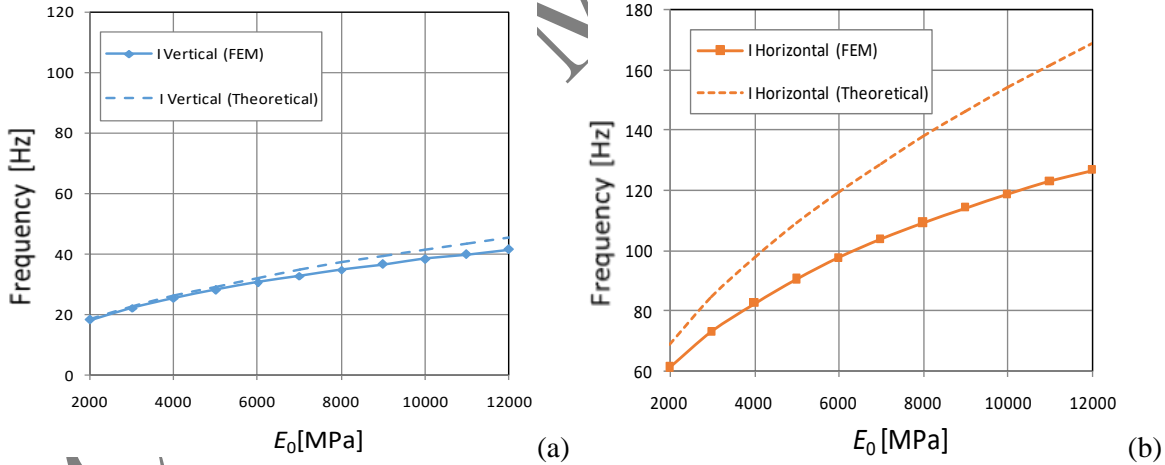
From a global examination of the results shown in Fig.4 and Fig.5, it can be concluded that first mode is influenced only by the modulus of elasticity parallel to the grain $E_0$, while the second vertical mode is affected by both $E_0$ and $G_{90}$. The torsional mode does not show any dependence

1  upon $E_0$, but is affected by the shear modulus, especially $G_0$. These conclusions can be effectively

2  used for the dynamic identification of the specimens according to the procedure described in the

3  next section.


4    3.3  *Comparison between the elementary beam theory and the sensitivity results*

5    As a first step, a comparison between Finite Element and Euler-Beam models has been carried

6  out as a way for understanding the limits of the beam theory applied in Eq.(1). Fig. 6 shows a

7  direct comparison between theoretical (Euler-Beam) and computational (FE) frequencies of the

8  first vertical and horizontal modes of the panel as a function of the modulus of elasticity $E_0$.

9    Figure 6 compares the theoretical and the computational frequency obtained respectively by

10  Eq.(1) and the FE model, showing the first vertical and horizontal natural frequencies of the panel

11  as function of the modulus of elasticity $E_0$.



12 (a)   (b)

13  **Fig. 6.** Comparison between theoretical and computed (FEM) natural frequencies of the first vertical and
14  the first horizontal bending mode of the panel, as function of the modulus of elasticity $E_0$: (a) first vertical
15  mode and (b) first horizontal mode.

16

17    It appears that Eq. (1) theoretical approach agrees well with the FE model for the first vertical

18  mode; on the other hand, a larger error affects the horizontal mode, leading to the conclusion that

19  the error provided by the use of Eq. (1) is not acceptable in the last case. This result can be easily

1 explained by the limitations of the Eq. (1), which is reliable when Euler-Bernoulli beam hypothesis

2 is fulfilled [16,43], namely in the case of high slenderness, whereby shear deformations are

3 negligible. As anticipated, for the considered horizontal mode, (low Length-to-Breadth ratio $L/B=$

4 4.4), shear contribution to deformations cannot be disregarded, when the rolling shear modulus of

5 the orthotropic material model is markedly low. This behavior is confirmed by Fig. 5a which

6 illustrates that the natural frequency of the horizontal mode is clearly influenced by the shear

7 modulus $G_0$. [44]. Nevertheless, the elementary beam theory can be effectively employed when

8 determining $E_0$ from the first vertical mode frequency in slender specimens [44].
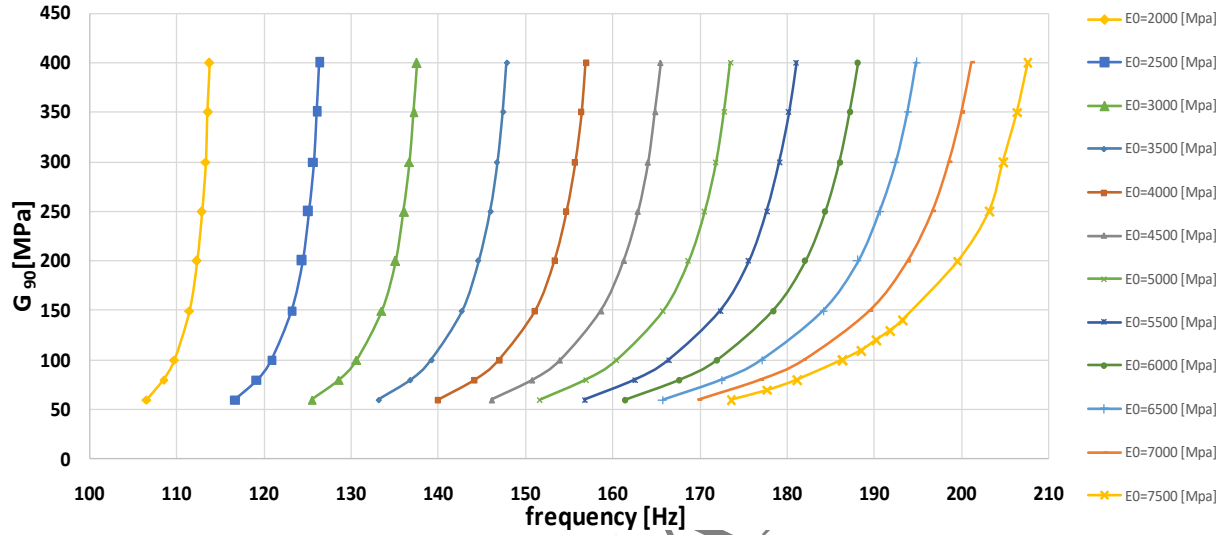
9     3.4 *Dynamic identification procedure (determination of $E_0$ and $G_{90}$)*

10     A dynamic identification procedure for the determination of the longitudinal MOE and rolling

11 shear modulus $G_{90}$ has been derived from the results of the sensitivity analyses conducted via the

12 FE model described in the previous Section. Various dynamic identification procedures have been

13 recently proposed by several authors [22,41,43]; these methodologies are based on Euler-Bernoulli

14 beam free vibration theory and are generally restricted to the evaluation of $E_0$ only.

15     The proposed approach mainly aims to extend the aforementioned procedures to the

16 determination of the rolling shear modulus $G_{90}$ of the specimen timber layers. As discussed in

17 Section 3.2, the three-layer panel dynamic behavior, in particular the vertical modes, is mainly

18 influenced by the elastic properties $E_0$ and $G_{90}$. A direct inspection of Fig. 5 (b) shows that, for a

19 predefined value of $E_0$ (= 7500 MPa), the second vertical mode frequency is directly related to the

20 rolling shear modulus $G_{90}$. A similar analysis has been carried out for discrete values of $E_0$, this

21 time restricted to a suitable range of 3500 to 7500 MPa, leading to the results shown in Fig.7,

22 where a second vertical mode sensitivity analysis is shown in terms of frequencies with respect to

1    *$G_{90}$*. For the sake of clearness, the axes of Fig.7 have been inverted with respect to the previous

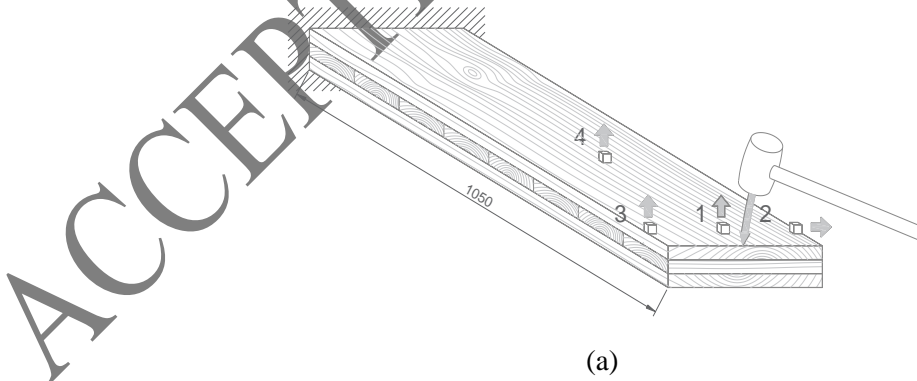2    Figs. 5-6 and a larger range of *$G_{90}$* has been considered.

3

4



5

6    **Fig. 7.** Rolling shear *$G_{90}$* as function of the frequency of the second vertical mode, for different values of
7                                       *$E_0$*.

8

9    The first step of the proposed procedure is therefore based on the determination of *$E_0$*   by means

10    of the sensitivity analysis approach displayed in Fig. 4a. As it can be deduced by Figs. 5-6, *$E_0$* is

11    sufficiently decoupled from the other elastic properties *$E_{90}$*, *$G_0$* and *$G_{90}$* for the given panel

12    configuration. It can therefore be independently calculated through the experimental evaluation of

13    the panel first mode frequency. The results are shown in Fig.4a. The second step requires the

14    experimental determination of the second vertical mode frequency of the specimen. Such trend,

15    evaluated by the FE modeling, has been plotted in Fig.7 as a function of *$G_{90}$* for different values

16    of *$E_0$*. Finally, the rolling shear modulus *$G_{90}$* is assessed, (see also section 3.6), after a proper

17    interpolation for the actual value of *$E_0$*. It is noteworthy that the above second step relies on the

18    hypothesis, discussed in section 3.2, that the second vertical mode frequency is hardly affected by

17

1  $G_0$ due to the high ratio $G_0/G_{90}$, which causes the shear deformations to mostly depend upon the

2  latter rolling shear modulus. An example of identification procedure applied to the 60PF-16

3  specimen is illustrated in section 3.6.


4  3.5  *Testing apparatus*

5  An experimental setup for the dynamic identification of the CLT panels has been prepared at

6  the laboratory of DICAAR, where a vibration test equipment has been assembled for the non-

7  destructive evaluation of the mechanical properties of the specimens (Fig. 8). Specimens have been

8  arranged in a cantilever configuration by fastening the fixed end to a rigid support through

9  appropriate clamps. In order to assess the effectiveness of the restraint, accelerations of the

10  clamped support have been carefully monitored in preliminary studies performed on the testing

11  apparatus, proving the reliability of the restraint assumptions. A proper impulsive mechanical load

12  has been subsequently applied to the specimen in order to selectively excite the different panel

13  vibration modes (Figs 8(a) and 8(b)).

14



15
16                                          (a)

18

(b)



(c)

**Fig. 8.** Testing apparatus for dynamic assessment of the 60PF specimens in cantilever bending scheme: (a) Schematic test and arrangement of accelerometers; (b) application of impulsive load, (c) Experimental set-up;

The vertical and horizontal accelerations have been detected by a set of #4 PCB 333B40 accelerometers whose properties are summarized in Table 4.

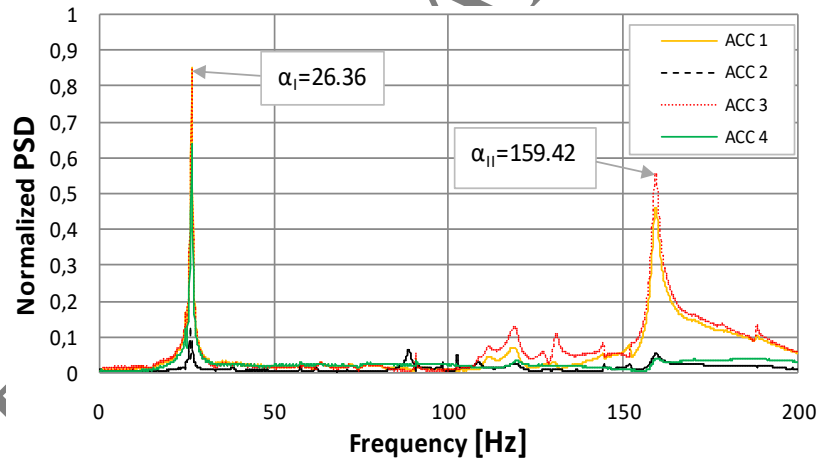▪ **Table 4**
▪ Properties of the PCB 333B40 accelerometers.

| Weight [gm] | Sensitivity [mV/g] | Frequency range [Hz] | Measurement Range [m/s²] |
|---|---|---|---|
| 7.50 | 500 | 0.5-3000 | ±98 |

▪

Accelerometers were located in proper positions on the specimen in the experimental setup shown in Fig.8. The distribution has been chosen in order to properly identify the modes of interest. For example, accelerometer #4 has been placed in the node of the second vertical mode (refer to Fig. 3(d) and Fig. 8), to identify the selected mode when almost zero amplitude is detected in the normalized Power Spectral Density PSD.

19

1    The signals have been acquired by the accelerometers through a data acquisition card and

2    processed by a LabVIEW-based software to directly elaborate the desired natural frequencies of

3    the panels. The software has been properly implemented to process vibrations signals, allowing

4    the determination of $E_0$ and $G_{90}$ according to the proposed procedure.

5    3.6  *Application of the identification procedure to a case study*

6    In the present section, the proposed dynamic identification procedure is illustrated for the 60-

7    PF16 specimen, however the same procedure has been repeated for all the remaining specimens.

8    As already mentioned, the procedure is based on the results of the sensitivity analyses conducted

9    by the FE model shown in Figs.4 and 5. The identification approach requires, as first step, the

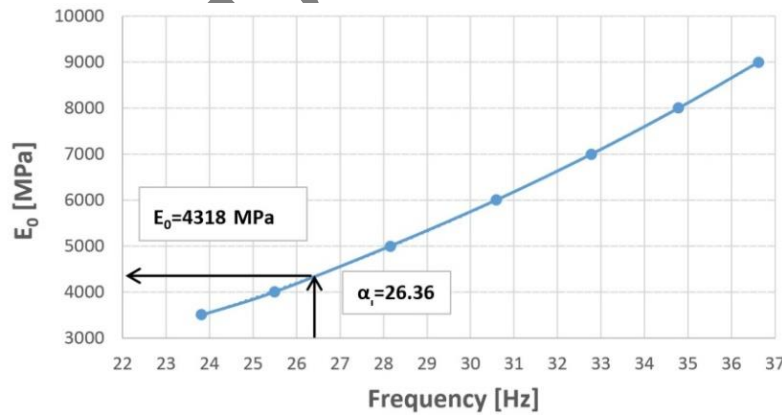10   determination of $E_0$ through the cantilever vibration method [43].



12   **Fig. 9.** Power Spectral Density response of the 60-PF16 panel.

13   Fig. 9 shows the normalized PSD function of the 60-PF16 panel specimen corresponding to a

14   mechanical impulse applied as illustrated in Fig. 8 and aimed at exciting vertical modes. The figure

15   highlights the first two vertical natural frequencies of the panel $\alpha_I$ and $\alpha_{II}$ needed for the

16   identification procedure.

1    It can be noted that the horizontal accelerometer #2 (see Fig.9) does not detect any evident peak.

2    Conversely similar trends of PSD are shown by accelerometers #1 and #3(see Figs.8a and 8c),

3    since the vertical mechanical impulse has been applied on the longitudinal symmetry axis of the

4    panel and no torsional mode has been excited.

5    Accelerometer #4 has been placed in proximity of the expected node of the second vertical

6    mode. Thus, as can be seen in Fig.9, the corresponding PSD does not highlight any evident peak

7    in correspondence of the second vertical natural frequency. Some "spurious" peaks are present as

8    well, displayed by accelerometer #3 in the interval between 100 and 150 Hz. These peaks have

9    been attributed to the torsional mode, slightly excited by small eccentricities of the mechanical

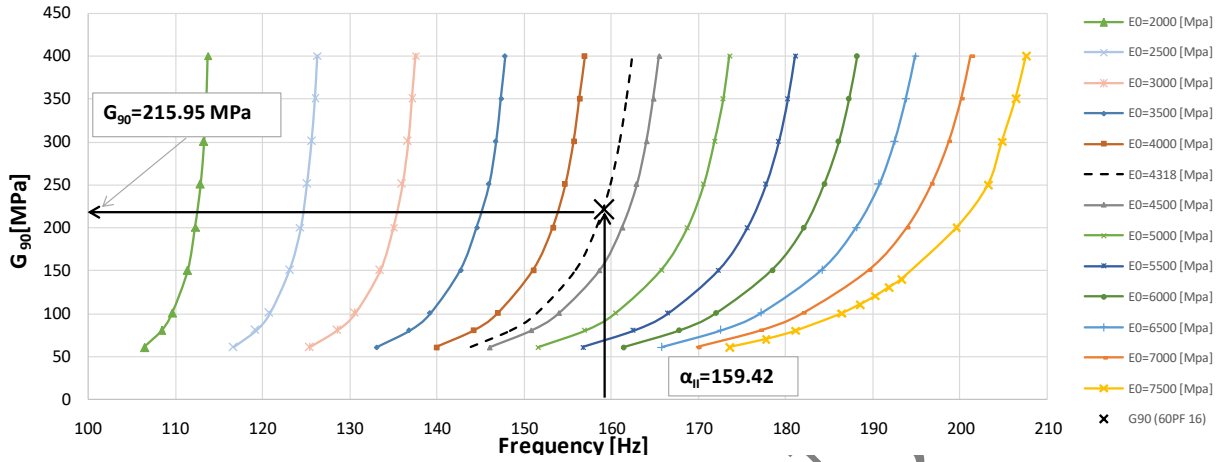10    impulse and/or by anatomic and geometric imperfections of the specimens.

11    The first frequency $\alpha_I$ is then processed for the determination of $E_0$ (Fig.10), which in the

12    present case results in a value of 4318 *MPa*.

13



15   **Fig. 10.** Illustrative example of the first step of the proposed dynamic identification procedure for the
16   determination of the modulus of elasticity $E_0$ of the 60-PF16 specimen.

17    Once $E_0$ has been evaluated, the second step requires a linear horizontal interpolation procedure

18    (Fig.11) leading to the dark dashed curve corresponding to the above measured $E_0$ of the panel

1 (60-PF16). A subsequent step allows the determination of $G_{90}$ for the considered specimen as a

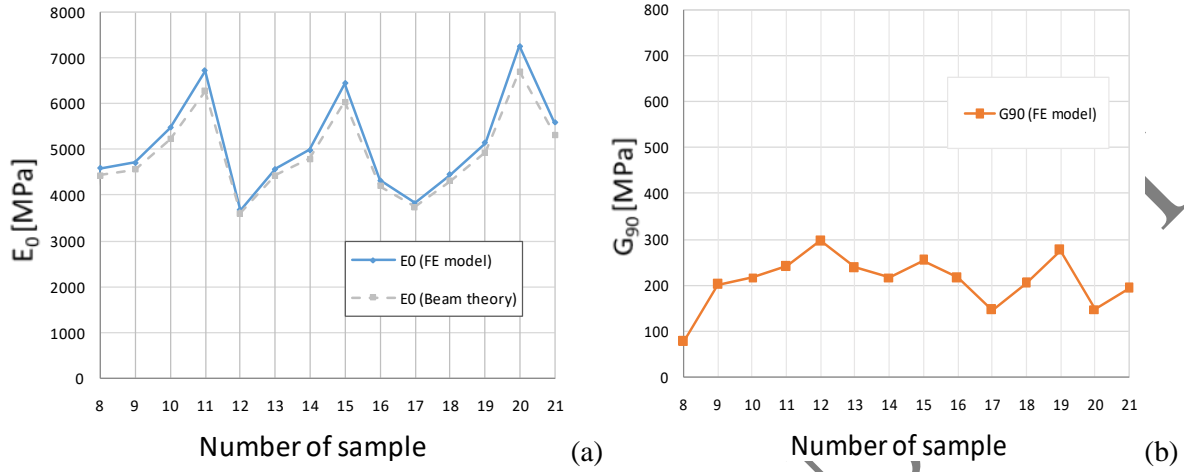2 function of the measured second vertical mode frequency $\alpha_{II}$ (Fig.11).



4 **Fig. 11.** Illustrative example of the second step of proposed dynamic identification procedure for the

5 determination of $G_{90}$ of the 60-PF16 panel with $E_0$= 4318 *MPa*

6     It should be noted (Fig. 11) that the proposed approach requires, especially for low values of

7 $E_0$, a high accuracy on $E_0$ [41,43,44], due to the high precision required by the horizontal

8 interpolation (dark dashed curve) and to the increasing slope of the curves for lower values of $E_0$.

9 **4. Results and discussion**

10     The above illustrated procedure has been used for a total of 14 3-layered CLT specimens made

11 of Sardinian Maritime Pine. The results obtained by means of the proposed identification technique

12 are discussed in the following. As mentioned in the previous section, the proposed technique relies

13 on the accuracy of the calculated $E_0$ which represents the starting point of the elaboration.

14 Therefore, for the purpose of evaluating the rolling shear modulus $G_{90}$, the use of FE model results

15 is strongly recommended for the first step of the proposed procedure. Moreover it has to be pointed

16 out that despite classic beam theory is commonly used to perform this task [41], the theoretical

1 approach tends to underestimate the elastic modulus $E_0$ by 4% for the considered 60-PF typology

2 (refer to Fig.12 and Table 5).



4 **Fig. 12.** Distribution of mechanical properties of the considered specimens, (a) Modulus of elasticity $E_0$,
5 (b) Rolling shear modulus $G_{90}$.

7     Results show a rather low Young's modulus $E_0$ than other softwood species [43,51,52], which

8 is not surprising given the low mechanical quality of the examined wood species. As previously

9 mentioned, a classification and the evaluation of the elastic properties of the boards forming the

10 panel has been already performed by the authors, e.g. [43,48,49] where a mean value of modulus

11 of elasticity of the panel boards forming the 60-PF specimens has been estimated as $E_0$=5190MPa

12 [43]; must be noted that such value matches very well the elastic modulus shown in Table 5

13 calculated by FE approach ($E_0$=5125.80 MPa). As previously anticipated (refer also to section 3.3),

14 such value differs by about 4% [41,44] from the elastic modulus calculated by classic beam theory

15 ($E_0$=4898.06MPa).

16 **Table 5**
17 Properties of the specimens: statistics (refer to Fig.12).

| Property | $\rho_0$ [kg/mc] | $E_0$ (beam theory) [MPa] | $E_0$ (FE) [MPa] | *Error* $E_0$[%] | $G_{90}$ (FE) [MPa] |
|---|---|---|---|---|---|
| Mean | 476.46 | 4898.06 | 5125.80 | -4.12% | 208.79 |

23

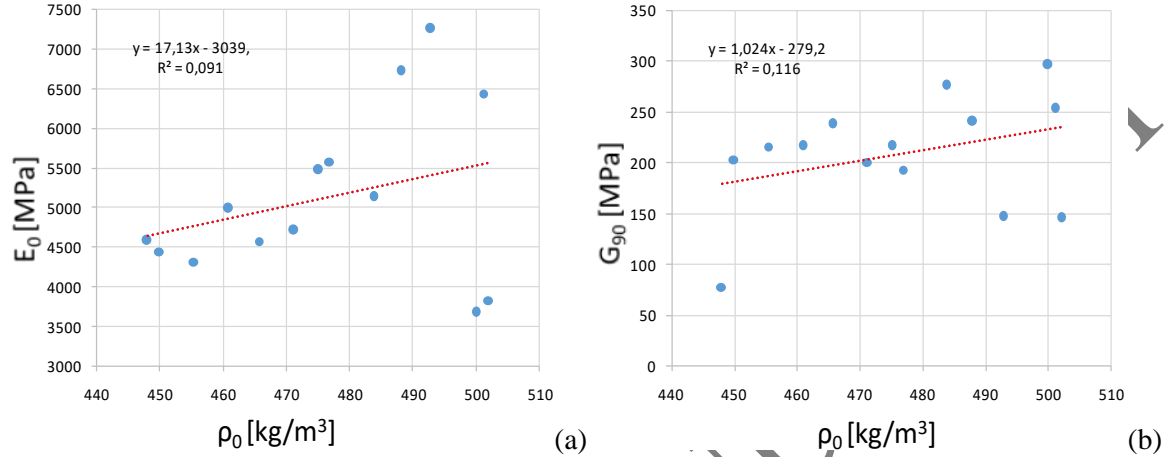| | | | | | |
|---|---|---|---|---|---|
| SD | 18.83 | 925.54 | 1067.88 | 0.02 | 56.55 |
| CV | 0.039 | 0.189 | 0.208 | -0.41 | 0.271 |

As displayed in Fig. 12 and Table 5, the rolling shear modulus shows the highest scatter, due to the influence of several parameters related to the intrinsic anisotropy of timber; e.g. Fellmoser and Blass [53] discussed the relationship between rolling shear modulus and strength and stiffness of timber elements; Görlacher [54] highlighted the influence of annual growth rings orientation on the value of $G_{90}$; Ehrhart et al. [55] identified in the sawing pattern and the boards geometry the main features affecting the rolling shear properties. These authors presented a comprehensive study summarizing the values of $G_{90}$ reported in literature for different European timber species including pine, confirming the high level of scattering of this parameter. Moreover, the study of Ehrhart et al. pointed out that European pine $G_{90}$ ranges between 90 MPa and 210MPa; it should be noted that, the values of rolling shear modulus reported in Fig.12b fall within this range, placing themselves towards its highest end. Thus, Sardinian maritime pine confirms a relatively high rolling shear modulus, if compared with other European species of pine.

It should be noted that the elastic properties evaluated using the proposed approach have to be considered as mean global properties of the panel. The proposed technique is therefore suitable for assessing the global behavior of the panel and may be conveniently exploited for CLT panel design and production control.

Figure 13 shows the correlation between the mean values of elastic properties $E_0$, $G_{90}$ and density $\rho_0$ for the tested specimens. It can be noted that both the correlations $\rho_0$-$E_0$ and $\rho_0$-$G_{90}$ are insignificant; this is consistent with similar results found by other authors ($R^2$=0.13) [55] for softwood species, especially for conifers, confirming the independence of elastic properties of Sardinian Maritime Pine of density. Better correlations were found in the case of hardwood

24

1    species; for example, in the cases of beech and ash, the correlation coefficient raise to $R^2$=0.34 and

2    $R^2$=0.50 respectively [55].

3



4

5    **Fig. 13.** Correlation between density and elastic properties of the considered specimens, (a) density vs
6    Modulus of elasticity $E_0$, (b) density vs rolling shear Modulus $G_{90}$.

7    ## 5. Summary and conclusions

8    In the present study, a new cantilever free vibration-based procedure has been introduced to

9    determine the elastic properties of a three-layer CLT panel made of Sardinian Maritime Pine.

10    The study has been focused on the determination of the Modulus of Elasticity $E_0$ and the Rolling

11    Shear Modulus $G_{90}$ of the boards composing the specimens, identified as the most significant

12    elastic properties for the examined panel layup.

13    The proposed procedure is based on the results of sensitivity studies conducted via FE model

14    analysis on a specific panel configuration. However the same approach could be easily extended

15    to any cantilever three-layer CLT specimen with different dimensions, provided that a new

16    sensitivity study is carried out for the new panel dimensions.

17    A straightforward relationship between the first two vertical mode frequencies of the CLT

18    panels and the elastic properties of their boards has been highlighted. The process enables a direct

comparison between the elastic properties and the corresponding free vibration frequencies of the panels. The elastic moduli $E_0$ and $G_{90}$ have been thus assessed for 14CLT specimens made of Maritime Pine, showing the possibility of replacing destructive static tests with non-destructive and quicker dynamic tests. In this respect, the proposed methodology has been proved to be an effective approach to assess the elastic properties of CLT panels in a straightforward way, which makes it a powerful tool to be used during quality control procedures in CLT manufacturing. More specifically, the proposed method focuses on the rolling shear modulus of the central layer of the specimen, whose direct experimental determination is more demanding.

The dynamic response of CLT specimens has been evaluated through a set of accelerometers suitably placed on the specimen surfaces. Alternatively, a faster and more effective data acquisition system based on laser sensor devices could be employed for a quality control procedure.

The discussed procedure assesses the average global elastic properties of the panels ($E_0$ and/or $G_{90}$) rather than local values, as addressed by standard procedures defined in European regulations. This approach somehow overcomes the scatter of elastic parameters at the local level, even within the same element, and the influence of defects, and thus represents a more useful evaluation.

Future studies will aim to possibly extend the proposed approach to the other elastic properties of CLT panels, e.g. $G_0$ or $E_{90}$, or to different panel layups (such as 5-layers CLT panels).

**Acknowledgements**

1 **References**

2 [1] Gagnon S, Pirvu C. CLT Handbook Cross-laminated Timber. Leesburg, Va: Erol
3       Karacabeyli, P.Eng., FPlnnovations, Brad Douglas, P.E., AWC 2013.

4 [2] Meloni D, Concu G, Valdés M, Giaccu GF. Fem models for elastic parameters
5       identification of cross laminated marittime pine panels. In: WCTE 2018. Seoul, Republic
6       of Korea.

7 [3] Vessby J, Enquist B, Petersson H, Alsmarker T. Experimental study of cross-laminated
8       timber wall panels. Eur. J. Wood Prod. 2009;67(2):211–218.

9 [4] Frangi A, Fontana M, Hugi E, Jübstl R. Experimental analysis of cross-laminated timber
10       panels in fire. Fire. Saf. J. 2009;44(8):1078–1087.

11 [5] Filiatrault A, Folz B. Performance-based seismic design of wood framed buildings J.
12       Struct. Eng. 2002;128(1):39–47.

13 [6] Schneider J, Stiemer SF, Tesfamariam S, Karacabeyli E, Popovski M. Damage assessment
14       of cross laminated timber connections subjected to simulated earthquake loads New
15       Zealand. In: WCTE Proceedings of the 12th world conference on timber engineering.
16       Auckland, New Zealand; 15-19 July 2012, 398-406.

17 [7] Buchanan A, Deam B, Fragiacomo M, Pampanin S, Palermo A. Multi-storey prestressed
18       timber buildings in New Zealand. Struct. Eng. Int. 2008;18(2):166–173.

19 [8] Kang W, Park B-D, Chung WY, Jung HS. Analytical modeling of rheological postbuckling
20       behavior of wood-based composite panels under cyclic hygro-loading. Wood Fiber Sci.
21       2003;35(3):409-420

22 [9] Bernasconi A, Corradi R, Galeazzi R. Experimental determination of out of plane elastic
23       shear modulus by three point bending test with varying span: Application to composite
24       laminates and particle wood panels In: ECCM - Proceeding of the 17th European
25       Conference on Composite Materials Munich, Germany.

26 [10] Rindler A, Vay O, Hansmann C, Müller U. Dimensional stability of multi-layered wood-
27       based panels: a review Wood Science and Technology 2017;51(5):969-996.

[11]   Davids WG, Rancourt DG, Dagher HJ. Bending performance of composite wood I-joist/oriented strand board panel assemblies. Forest Products Journal 2011;61(3)(3):246-256

[12]   Norris AN. Flexural waves on narrow plates. J Acoust Soc Am 2003;113(5):2647–2658.

[13]   Hu L, Gagnon S. Controlling cross-laminated timber (CLT) floor vibrations–fundamentals and method. In: World Conference on Timber Engineering. 269–275.

[14]   Öqvist R, Ljunggren F, Ågren A. Variations in sound insulation in cross laminated timber housing construction. In: Forum Acusticum. Aalborg, Denmark.

[15]   Schoenwald S, Zeitler B, Sabourin I, King F. Sound insulation performance of cross laminated timber building systems. In: Proceedings of Internoise, 42nd international congress and exposition on noise control engineering. Innsbruck, Austria.

[16]   Christovasilis IP, Brunetti M, Follesa M, Nocetti M, Vassallo D. Evaluation of the mechanical properties of cross laminated timber with elementary beam theories. Const. Build. Mater. 2016;122:202-213.

[17]   Glišović I, Pavlović M, Stevanović B, Todorović M. Numerical analysis of glulam beams reinforced with CFRP plates. Journal of Civil Engineering and Management 2017;Volume 23, Issue 7, 3 October 2017, Pages 868-879(7):868-879.

[18]   Tran T-T, Thi V-D, Khelifa M, Oudjene M, Rogaume Y. A constitutive numerical modelling of hybrid-based timber beams with partial composite action Construction and Building Materials 2018;178:462-472.

[19]   Bedon C, Fragiacomo M. Numerical analysis of timber-to-timber joints and composite beams with inclined self-tapping screws. Composite Structures 2019;207:13-28.

[20]   Fellmoser P, Blass H. Influence of rolling shear modulus on strength and stiffness of structural bonded timber elements. In: CIB-W18 Meeting.

[21]   Schubert SI, Gsell D, Dual J, Motavalli M, Niemz P. Rolling shear modulus and damping factor of spruce and decayed spruce estimated by modal analysis. Holzforschung 2006;60:78–84.

[22] Van Damme B, Schoenwald S, Armin Z. Modeling the bending vibration of cross-laminated timber beams Eur. J. Wood Prod. 2017;75:985–994

[23] Thiel A, Schickhofer G. CLT designer – A software tool for designing cross laminated timber elements: 1D-plate-design. In: 11th World Conference on Timber Engineering. Riva del Garda, Italy.

[24] EN-1995:2008-06 Eurocode 5: Design of timber structures – Part 1-1: General – Common rules and rules for buildings. European Standard, European Committee for standardization

[25] Blass HJ, Fellmoser P. Design of solid wood panels with cross layers. In: Proceedings of CIB - W18 timber engineering. Lathi, Finland, 543-548.

[26] Kreuzinger H. Platten, Scheiben und Schalen. Ein Berechnungsmodell für gängige Statikprogramme. Bauen mit Holz 1999;1:34 - 39.

[27] Kaci A, Houari & M.S.A., A. Bousahla, Tounsi A, Hassan S. Post-buckling analysis of shear-deformable composite beams using a novel simple two-unknown beam theory- • March 2018. Structural Engineering & Mechanics 2018;65(5):621-631.

[28] Draiche K, Tounsi A, Mahmoud SR. A refined theory with stretching effect for the flexure analysis of laminated composite plates. Geomechanics and Engineering 2016;11(5):671-690.

[29] Bakhadda B, Bachir Bouiadjra M, Bourada F, Anis Bousahla A, Tounsi A, Mahmoud SR. Dynamic and bending analysis of carbon nanotube-reinforced composite plates with elastic foundation Wind and Structures;27(5):311-324.

[30] Belabed Z, Anis Bousahla A, Sid Ahmed Houari M, Tounsi A, Mahmoud SR. A new 3-unknown hyperbolic shear deformation theory for vibration of functionally graded sandwich plate. Earthquakes and Structures 2018;14(2):103-115.

[31] Zidi MH, M.S.A. & Tounsi, A. & Bessaim, A. & Hassan S. A novel simple two-unknown hyperbolic shear deformation theory for functionally graded beams. Structural Engineering & Mechanics 2017;64(2):145-153.

1 [32] A. Zine, A. Tounsi, K. Draiche, Sekkal M, Mahmoud SR. A novel higher-order shear
2 deformation theory for bending and free vibration analysis of isotropic and multilayered
3 plates and shells Steel and Composite Structures 2018;26(2):125-137.

4 [33] Chikh A, Tounsi A, Hebali H, Mahmoud SR. Thermal buckling analysis of cross-ply
5 laminated plates using a simplified HSDT Smart Structures and Systems 2017;19(3):289-
6 297.

7 [34] Mokhtar Y, Heireche H, Bousahla AA, (...), Tounsi A, Mahmoud SR. A novel shear
8 deformation theory for buckling analysis of single layer graphene sheet based on nonlocal
9 elasticity theory. Smart Struct. Syst. 2018;21(4):397-405.

10 [35] Houari MSA, Tounsi A, Bessaim A, Mahmoud SR. A new simple three-unknown
11 sinusoidal shear deformation theory for functionally graded plates. Steel and Composite
12 Structures 2016;22(2):257-276.

13 [36] Mouffoki A, Adda Bedia EA, Houari MSA, Tounsi A, Mahmoud SR. Vibration analysis
14 of nonlocal advanced nanobeams in hygrothermal environment using a new two-unknown
15 trigonometric shear deformation beam theory. Smart Struct. Syst. 2017;20(3):369-383.

16 [37] Steiger R, Gülzow A, Czaderski C, Howald MT, Niemz P. Comparison of bending stiffness
17 of cross-laminated solid timber derived by modal analysis of full panels and by bending
18 tests of strip-shaped specimens. Eur J Wood Prod 70 2011;70(1-3):141-153.

19 [38] Keunecke D, Sonderegger W, Pereteanu K, Lüthi T, Niemz P. Determination of Young's
20 and shear moduli of common yew and Norway spruce by means of ultrasonic waves. Wood
21 Sci Technol 2006;41(4):309–327.

22 [39] Dahmen S, Ketata H, Ben Ghozlen MH, Hosten B. Elastic constants measurement of
23 anisotropic Olivier wood plates using aircoupled transducers generated Lamb wave and
24 ultrasonic bulk wave. Ultrasonics 2010;50(4-5):502-507.

25 [40] Gonçalves R, Trinca A, Pellis BP. Elastic constants of wood determined by ultrasound
26 using three geometries of specimens. Wood Sci Technol 2014;48:269-287.

27 [41] Guan C, Zhang H, Zhou L, Wang H. Dynamic determination of modulus of elasticity of
28 full-size wood composite panels using a vibration method. Construction and Building
29 Materials 2015;100:201-206.

[42]   Guan C, Zhang H, Hunt JF, Yan H. Determining shear modulus of thin wood composite materials using a cantilever beam vibration method. Construction and Building Materials 2016;121:285-289.

[43]   Giaccu GF, Meloni D, Valdès M, Fragiacomo M. Dynamic determination of modulus of elasticity of maritime pine cross-laminated panels using vibration methods. In: Sustainable Development and Planning IX .WIT Transactions on Ecology and The Environment WIT Press New Forest, UK; 2017, 571-579.

[44]   Giaccu GF, Meloni D, Concu G, Valdés M. Considerations on dynamic identification of wood composite panels using a cantilever beam vibration method. In: WCTE 2018. Seoul, Republic of Korea; August 20-23.

[45]   EN-408:2012-07 Timber structures – Structural timber and glued laminated timber – Determination of some physical and mechanical properties. European Standard, European Committee for standardization,

[46]   Meirovitch L. Analytical methods in vibrations. New York: The Macmillan Company, 1967.

[47]   EN 338:2009–10 Structural timber – Strength classes. European Standard, European Committee for standardization,

[48]   Riu R. Caratterizzazione di pannelli XLam in Pino Marittimo sardo. University of Cagliari, Italy; 2016.

[49]   Concu G, Fragiacomo M, Trulli N, Valdes M. Grading of Maritime Pine from Sardinia (Italy) for use in cross-laminated timber. In: Proceedings of the Institution of Civil Engineers - Construction Materials. 2017, 11-12.

[50]   EN 384+A1 Structural timber - Determination of characteristic values of mechanical properties and density European Standard, European Committee for standardization, 2018.

[51]   Yang N, Zhang L. Investigation of elastic constants and ultimate strengths of Korean pine from compression and tension tests. Journal of Wood Science 2018;64(2):85-96.

1  [52]  Daoui A, Zerizer A. Identification of elasticity modulus by vibratory analysis (Application
2         to a natural composite: Aleppo pine wood). In: 2nd International Congress on Materials
3         and Structural Stability, CMSS 2017. Rabat; Morocco; 22-25 November 2017.

4  [53]  Fellmoser P, Blass HJ. Influence of Rolling Shear Modulus on Strength and Stiffness of
5         Structural Bonded Timber Elements. In: Edinburgh, United Kingdom.

6  [54]  Gorlacher R. Ein verfahren zur ermittlung des rollschubmoduls von holz. Universität
7         Karlsruhe (TH) 2002.

8  [55]  Ehrhart T, Brandner R, Schickhofer G, Frangi A. Rolling Shear Properties of Some
9         European Timber Species with Focus on Cross Laminated Timber (CLT): Test
10        Configuration and Parameter Study. In: International Network on Timber Engineering
11        Research (INTER 2015). Šibenik, Croatia.